

This article was downloaded by:

On: 14 January 2011

Access details: *Access Details: Free Access*

Publisher *Taylor & Francis*

Informa Ltd Registered in England and Wales Registered Number: 1072954 Registered office: Mortimer House, 37-41 Mortimer Street, London W1T 3JH, UK



## Molecular Simulation

Publication details, including instructions for authors and subscription information:

<http://www.informaworld.com/smpp/title~content=t713644482>

### Compact modeling of the threshold voltage in silicon nanowire MOSFET including 2D-quantum confinement effects

J. L. Autran<sup>a</sup>; K. Nehari<sup>a</sup>; D. Munteanu<sup>a</sup>

<sup>a</sup> L2MP, UMR CNRS 6137, Bâtiment IRPHE, Marseille Cedex 13, France

**To cite this Article** Autran, J. L. , Nehari, K. and Munteanu, D.(2005) 'Compact modeling of the threshold voltage in silicon nanowire MOSFET including 2D-quantum confinement effects', *Molecular Simulation*, 31: 12, 839 — 843

**To link to this Article:** DOI: 10.1080/08927020500314027

**URL:** <http://dx.doi.org/10.1080/08927020500314027>

PLEASE SCROLL DOWN FOR ARTICLE

Full terms and conditions of use: <http://www.informaworld.com/terms-and-conditions-of-access.pdf>

This article may be used for research, teaching and private study purposes. Any substantial or systematic reproduction, re-distribution, re-selling, loan or sub-licensing, systematic supply or distribution in any form to anyone is expressly forbidden.

The publisher does not give any warranty express or implied or make any representation that the contents will be complete or accurate or up to date. The accuracy of any instructions, formulae and drug doses should be independently verified with primary sources. The publisher shall not be liable for any loss, actions, claims, proceedings, demand or costs or damages whatsoever or howsoever caused arising directly or indirectly in connection with or arising out of the use of this material.

# Compact modeling of the threshold voltage in silicon nanowire MOSFET including 2D-quantum confinement effects

J. L. AUTRAN\*†, K. NEHARI and D. MUNTEANU

L2MP, UMR CNRS 6137, Bâtiment IRPHE, 49 rue Joliot-Curie, BP 146, F-13384, Marseille Cedex 13, France

(Received June 2005; in final form August 2005)

A quantum-mechanical compact model of the threshold voltage ( $V_T$ ) for quantum nanowire MOSFETs has been developed. This approach is based on analytical solutions for the decoupled 2D Schrödinger and 1D Poisson equations solved in the silicon channel. A quantum correction based on the perturbation theory has been also introduced to improve the model accuracy. Finally, the validity of the model has been verified by comparison with data obtained with a 2D/3D Poisson-Schrödinger drift-diffusion simulation code.

**Keywords:** Compact modeling; Threshold voltage; Quantum nanowire MOSFET; 2D-quantum confinement effects; 3D numerical simulation

## 1. Introduction

Multi-gate MOS transistors are widely recognized as one of the most promising solutions for meeting the roadmap requirements in the deca-nanometer scale of device integration [1]. Recently, these architectures are also presenting a growing interest for the integration of post-conventional Silicon devices and molecular-based devices, since the active region of the transistor, i.e. the conduction channel, can be alternatively played by a semiconductor nanowire, a Carbon nanotube, a molecule or an atomic linear chain [2,3]. In all cases, these structures exhibit a superior control of short channel effects resulting from an exceptional electrostatic coupling between the conduction channel and the surrounding gate electrode.

In the case of Silicon-based CMOS technologies, a wide variety of multi-gate architectures, including Double-Gate (DG), Gate-All-Around (GAA), PiFET, FinFET, Rectangular or Cylindrical nanowire MOSFETs, linear atomic-chain transistors has been proposed in the recent literature [1,2]. For all these structures, one of the identified challenges remains the development of compact models taking into account the main physical phenomena governing the devices at this scale of integration.

In this work, a compact model for the threshold voltage ( $V_T$ ) of long-channel quantum Si nanowire (QW) MOSFETs is developed. Schematic representations of different QW architectures are shown in figure 1. In such devices for which the lateral dimensions, i.e. the Si film thickness and its width, are ultimately downscaled to a few nanometers, quantum-mechanical carrier confinement effects are exacerbated in the two ( $y$ - and  $z$ -) directions perpendicular to the transport one ( $x$ -). As we will detail in the following, our present approach is thus based on the decoupled solution of the Poisson and Schrödinger equations in the ( $y, z$ ) plane of the structure. Threshold voltage obtained from this new model will be confronted with data directly calculated using a 2D/3D quantum-mechanical simulation code coupling the Poisson-Schrödinger system with the Drift-Diffusion transport equation (Balmos3D).

## 2. Threshold voltage modeling

### 2.1 $V_T$ definition and criterion

The band diagram in the vertical ( $y$ -) direction (middle of the structure) for a n-channel QW transistor is

\*Corresponding author. Email: autran@newsup.univ-mrs.fr

†Also with the Institut Universitaire de France—IUF

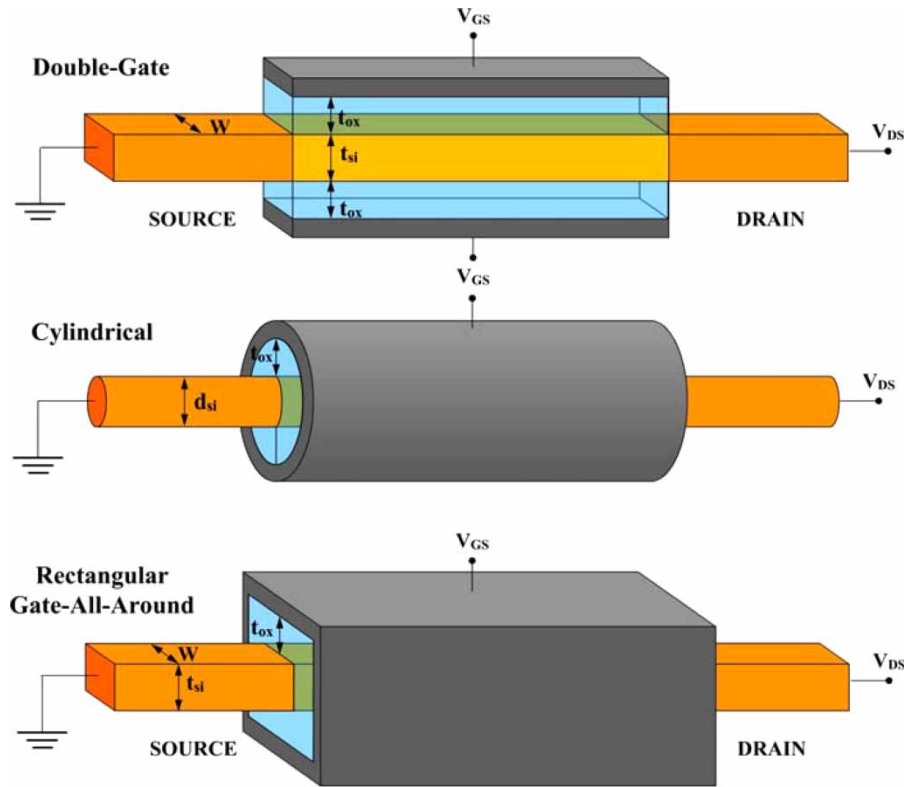


Figure 1. Schematic representation of different architectures envisaged for the Si nanowire MOSFET. The main geometrical key-parameters of the devices are defined.

schematically shown in figure 2. The potential reference is assumed to be the electron Fermi level of the n+ source region. The potential,  $\Psi$ , is defined as the band bending with respect to the intrinsic Fermi level in the silicon film. It is important to note that the surface potential,  $\Psi_s$ , as defined here, is different from the surface potential in conventional bulk MOSFET,  $\Psi_{sc}$ , which is given by the band bending between the silicon surface and the substrate volume. The relation between the two potentials is  $\Psi_{sc} = \Psi_s + \phi_F$  where  $\phi_F = (kT/q) \ln(N_A/n_i)$  is the Fermi potential,  $N_A$  is the film doping and  $n_i$  is the intrinsic carrier concentration. In conventional MOSFET, the

threshold voltage is usually defined as the gate voltage necessary for obtaining a band bending of  $\Psi_{sc} = 2\phi_F$ , which means  $\Psi_s = \phi_F$ . This definition does no more apply to QW MOSFET: our extensive numerical simulation fully confirms this remark and shows that surface potential at threshold,  $\Psi_s^T$ , is different from  $\phi_F$ . Other definitions for  $V_T$  exist, as derived from the constant-current method or the maximum of  $\partial^2 I_D / \partial V_G^2$ . In a recent work [4], we used this latter criterion, but the resulting analytical expression of the threshold voltage is quite complicated and its demonstration demands heavy mathematical manipulations. For obtaining a more simple expression of  $V_T$ , we consider here the well-known definition where  $V_T$  is the gate voltage for which the inversion charge  $Q_{iT}$  in the transistor channel (inversion charge at threshold) is given by [4,5]:

$$Q_{iT} \equiv (V_G - V_T)C_{ox} = \frac{kT}{q} C_{ox} \quad (1)$$

where  $V_G - V_T$  is assumed to be  $\sim kT/q$  around threshold. We verified that this value of  $Q_{iT}$  is very close to the inversion charge obtained by the numerical simulation of multi-gate structures with different channel doping levels, channel thicknesses and gate oxide thicknesses.

Once the inversion charge at threshold has been defined, the determination of  $V_T$  can be easily conducted in two steps: (i) express this inversion charge ( $Q_i$ ) in the QW channel as a function of  $V_G$  and (ii) numerically solve the equation  $Q_i(V_G) = Q_{iT}$ . In the following, the calculation

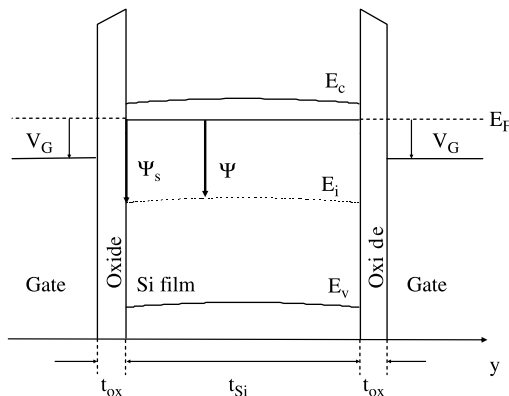


Figure 2. Schematic band diagram for a QW transistor in the y-direction (middle part of the device) and definition of internal potential and energy levels.

of  $Q_i$  is obtained from the decoupled solution of the Poisson and Schrödinger equations. The first equation leads to the band bending profile in the Si film; the second one gives energy levels in the QW (considered as a 2D quantum-well) used to evaluate the inversion charge.

## 2.2 Device electrostatics

Considering a multi-gate QW structure shown in figure 1, our approach is based on a parabolic approximation of the vertical (y-) potential distribution in the film at threshold, which has been fully confirmed by numerical simulation in previous studies [4,6]. This result can be, of course, generalized for the other direction (z-axis) perpendicular to the channel axis. We can write:

$$\Psi = \Psi_s - \beta t_{Si} y + \beta y^2 \quad (2)$$

With definitions in figure 1 and applying the Gauss law, the boundary conditions at the two oxide/silicon interfaces are identical and give:

$$V_G - V_{FB} = \frac{\epsilon_{Si}}{\epsilon_{ox}} t_{ox} E + \Psi_s + \phi_F \quad (3)$$

where  $V_{FB}$  is the flat band voltage,  $\epsilon_{Si}$  and  $\epsilon_{ox}$  are the silicon and oxide permittivities, respectively,  $t_{ox}$  is the oxide thickness and  $E$  is the electric field at the interface:

$$E = - \left. \frac{d\Psi}{dy} \right|_{y=0} = \beta t_{Si} \quad (4)$$

Expressions (2)–(5) form a complete set of equations to analytically evaluate the band bending profile in the silicon film under threshold condition. As shown in figure 3 in comparison with numerical simulation, equation (2) is a very good approximation for the potential distribution in the film at threshold for various doping levels. The potential is symmetric with respect to the middle of the silicon film and has a quasi-parabolic dependence.

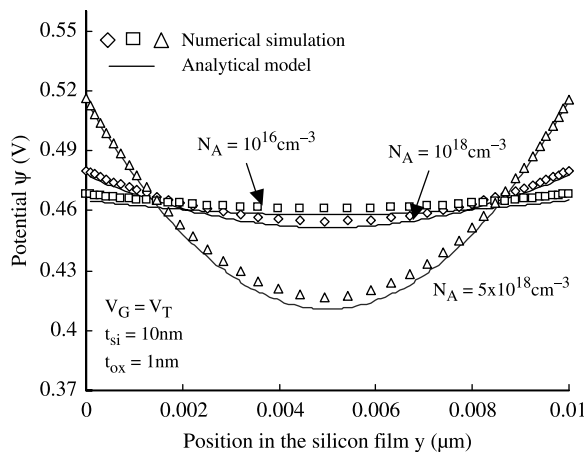


Figure 3. Potential distribution in the silicon film at threshold in a symmetric DG-QW structure for different doping levels as calculated by the analytical model and numerically solved from Poisson equation.

## 2.3 Quantum-mechanical evaluation of the inversion charge

The second step of our model consists in calculating the inversion charge in the silicon quantum-wire. In a first approach, this QW can be simply depicted as a 2D quantum-well with infinite walls, for example, a rectangular well for DG or GAA structures, a cylindrical well for the cylindrical QW transistor (figure 1), etc. The calculations are developed here for the rectangular infinite well (i.e. the GAA structure) with carriers confined in the (y, z) plane. Assuming, in a first approximation, that the conduction band profile is flat inside the well, simple analytical expression for the quantum energy levels can be used. In the particular case of  $\langle 100 \rangle$ -oriented Silicon, three different series of quantum energy levels must be considered in the evaluation of the inversion charge, to properly take into account the effective mass ellipsoid characteristics (figure 4):

$$\begin{cases} E_1(i, j) = \frac{\pi^2 \hbar^2 i^2}{m_l t_{Si}^2} + \frac{\pi^2 \hbar^2 j^2}{m_t W^2} \\ E_2(i, j) = \frac{\pi^2 \hbar^2 i^2}{m_t t_{Si}^2} + \frac{\pi^2 \hbar^2 j^2}{m_l W^2} \\ E_3(i, j) = \frac{\pi^2 \hbar^2 i^2}{m_t t_{Si}^2} + \frac{\pi^2 \hbar^2 j^2}{m_t W^2} \end{cases} \quad (5)$$

where  $m_l \approx 0.916 \times m_0$  and  $m_t \approx 0.19 \times m_0$  are the longitudinal and transversal effective mass of electrons, respectively.

For each energy level  $E_k(i, j)$ , referenced with respect to the bottom of the quantum-well, the contribution to

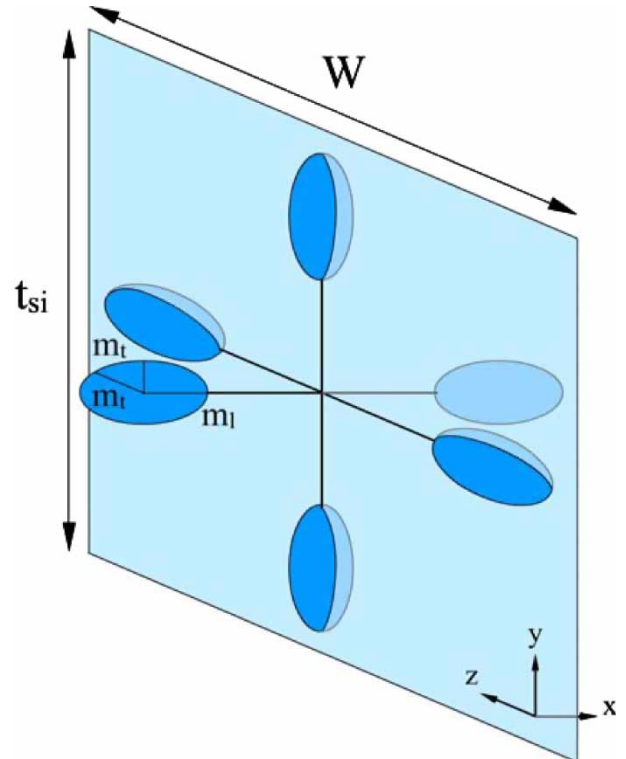


Figure 4. Schematic illustration of electron confinement in a Silicon quantum-wire with a rectangular cross-section ( $W \times t_{Si}$ ).

the total charge integrated over the Si film cross-section ( $W \times t_{\text{Si}}$ ) is:

$$n(E_k, i, j) = 2 \int_{E_k}^{+\infty} \rho_{1D}(E, E_k) f(E) dE \quad (6)$$

where the factor 2 accounts for the number of equivalent valleys,  $\rho_{1D}(E, E_k)$  is the 1D density-of-states and  $f(E)$  is the Fermi-Dirac distribution function:

$$\rho(E, E_k) = \frac{1}{\pi} \left( \frac{2m_D}{\hbar^2} \right)^{1/2} \frac{1}{\sqrt{E - E_k}} \quad (7)$$

$$f(E) = \frac{1}{1 + \exp\left(\frac{E - E_F}{kT}\right)} \quad (8)$$

where  $m_D$  is the 1D density-of-states effective mass ( $m_D = m_t$  for  $k = 1, 2$  and  $m_D = m_l$  for  $k = 3$ ).

In equation (6), the calculated charge depends on  $V_G$  via the position of the Fermi level with respect to the bottom of the conduction band (assimilated to the bottom of the quantum well) and thus with respect to the different energy levels. The inversion charge to be considered for  $V_T$  determination using  $Q_i(V_G) = Q_i^T$  is finally:

$$Q_i(V_G) = q \sum_k \sum_i \sum_j n(E_k, i, j) \quad (9)$$

In order to enhance the accuracy of the model, a first-order perturbation correction of the energy levels given by equation (5) has been conducted [6,7]. The Hamiltonian  $V$  of the perturbation is simply evaluated from the electrostatic potential profile (equation (2)), assuming that a similar profile is obtained in the second perpendicular direction (figure 5):

$$V(y, z) = \beta_y y(t_{\text{Si}} - y) + \beta_z z(W - z) \quad (10)$$

where  $\beta_y$  and  $\beta_z$  are two constants depending on  $\beta$ .

The first-order correction to apply to the energy levels in the well is given by:

$$\Delta E^{i,j} = \langle \varphi^{i,j} | V | \varphi^{i,j} \rangle \quad (11)$$

with  $\varphi^{i,j}$  is the wave function related to levels defined with quantum numbers  $i$  and  $j$ :

$$\varphi^{i,j}(y, z) = \sqrt{\frac{2}{t_{\text{Si}}}} \sin\left(\frac{i\pi y}{t_{\text{Si}}}\right) \cdot \sqrt{\frac{2}{W}} \sin\left(\frac{j\pi z}{W}\right) \quad (12)$$

An analytical evaluation of  $\Delta E^{i,j}$  immediately gives:

$$\begin{aligned} \Delta E^{i,j} &= \iint_{W \times t_{\text{Si}}} [\varphi^{i,j}(y, z)]^2 V(y, z) dy dz \\ &= \frac{\beta_y t_{\text{Si}}^2}{6} \left(1 + \frac{3}{i^2 \pi^2}\right) + \frac{\beta_z W^2}{6} \left(1 + \frac{3}{j^2 \pi^2}\right) \end{aligned} \quad (13)$$

The corrected energy levels to be considered in equation (9)

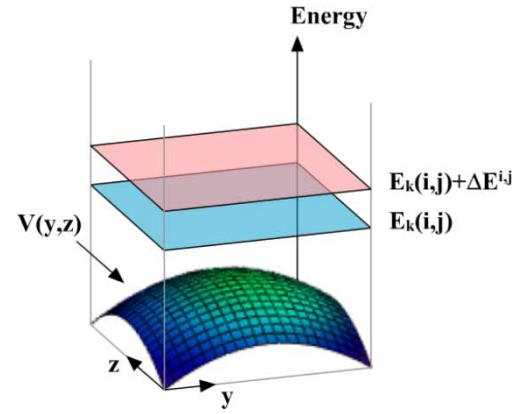


Figure 5. Illustration of the first-order perturbation method used to correct energy level values in the 2D rectangular well of the QW MOSFET.

for the evaluation of  $Q_i$  are finally:

$$\tilde{E}_k(i, j) = E_k(i, j) + \Delta E^{i,j} \quad (14)$$

### 3. Model validation and discussion

The present model has been validated by comparison with numerical simulation using a 2D/3D quantum-mechanical simulation code coupling the Poisson–Schrödinger system with the Drift-Diffusion transport equation (Balmos3D, [8]). First, considering a single direction for carrier confinement ( $t_{\text{Si}}$  downscaling at fixed infinitely large  $W$ ). Figure 6 shows that a very good match is obtained between analytical and 2D numerical results in a rectangular QW structure. In particular, it is shown that the model is able to very well predict the dependence of  $V_T$  with  $t_{\text{Si}}$  and also with  $N_A$ . In a second step, both  $y$ - and  $z$ -directions for carrier confinement have been considered and the compact model has been validated using 3D numerical simulation, as shown in figure 7. Once again the fit between compact model and numerical data is very satisfactory. Figures 7 and 8 show that the threshold voltage increase, due to carrier confinement in the  $z$ -direction, becomes significant for  $W$  lower than  $\sim 20$  nm. It is also interesting to remark that, when  $W$  is scaled down, the

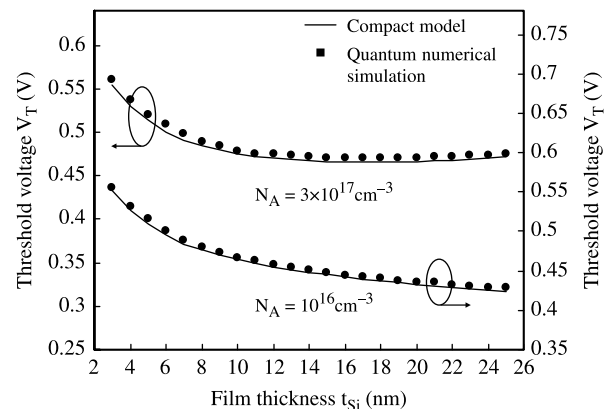


Figure 6. Quantum  $V_T$  predicted by the analytical model in an infinitely large DG-QW structure for two different doping levels. Comparison with 2D quantum-mechanical numerical simulation is also reported.



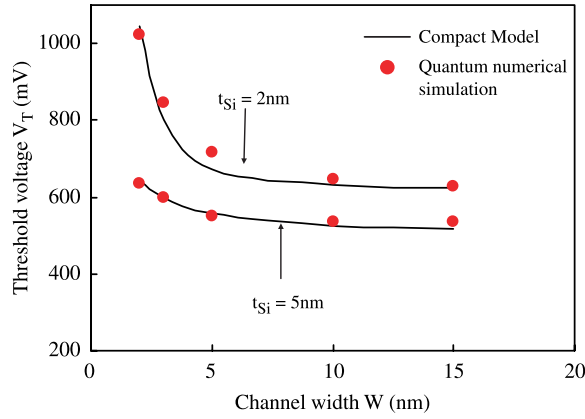


Figure 7. Quantum  $V_T$  predicted by the analytical model as a function of  $W$  and  $t_{Si}$  for a rectangular GAA QW. Comparison with 3D quantum numerical simulation.

threshold voltage increase becomes more important as long as the film thickness decreases. Indeed, when switching from 1D to 2D confinement, the threshold voltage increase is more pronounced due not only to the increase of the distance between the energy levels and the Fermi level, but in the same time, to the change of the density-of-states. In other words, the band bending must be accentuated to obtain the same inversion charge with higher energy levels and lower number of quantum states per level. Finally, figure 9 shows the variations of  $V_T$  predicted by the compact model as a function of both  $W$  and  $t_{Si}$  for a rectangular GAA QW.

#### 4. Conclusion

In conclusion, a compact modeling of the threshold voltage for quantum-wire MOSFETs has been developed. The

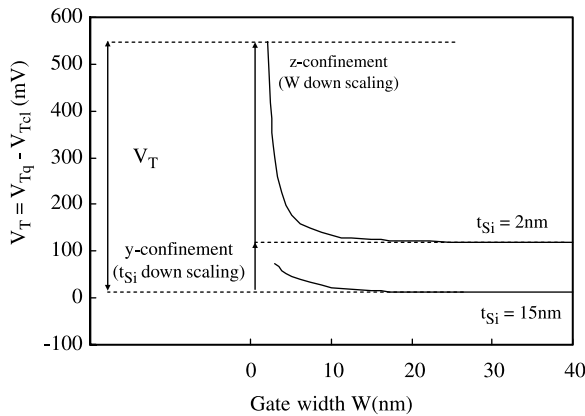


Figure 8.  $\Delta V_T$  predicted by the analytical model as a function of the channel width in thick and very thin films, illustrating the contributions of 1D and 2D confinements in the threshold voltage shift between quantum ( $V_{Tq}$ ) and classical ( $V_{Tcl}$ ) threshold voltage.

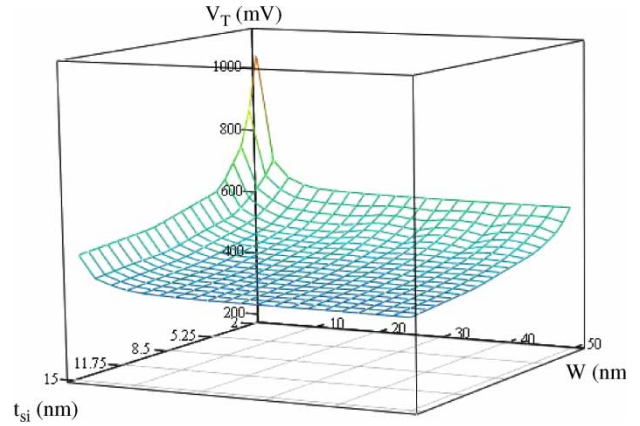


Figure 9.  $V_T(W, t_{Si})$  surface map for a rectangular GAA QW long-channel transistor ( $L = 100$  nm,  $V_{DS} = 50$  mV,  $N_A = 10^{16}$  cm $^{-3}$ ) as calculated by the proposed model.

model, based on analytical solutions for the decoupled Schrödinger and Poisson equations, also integrates a quantum correction based on the perturbation theory to improve the evaluation of the inversion charge in the film. The validity of this approach has been demonstrated by comparison with 3D numerical simulation. Finally this work provides an analytical and useful way for the threshold voltage evaluation in such nanodevices with a unified formalism employed in both classical and quantum-mechanical approaches.

#### Acknowledgements

This work is supported by the European Commission in the framework of the Network of Excellence on Silicon-based nanodevices (SINANO, contract IST-506844).

#### References

- [1] For a recent review, see D. Hisamoto, Short course IEDM 2003 and references therein.
- [2] M. Bescond, *et al.* 3D quantum modeling and simulation of multiple-gate nanowire MOSFETs. *IEDM Tech. Dig.*, 617 (2004).
- [3] M. Bescond, *et al.* Atomic-scale modeling of Double-Gate MOSFETs using a tight-binding Green's function formalism. *Solid-State Electron.*, **48**, 567 (2004).
- [4] D. Munteanu, *et al.* Unified analytical model of threshold voltage in symmetric and asymmetric Double-Gate MOSFETs. *Proc. ULIS*, 35 (2003).
- [5] S. Harrison, *et al.* Electrical characterization and modelling of high-performance SON DG MOSFETs. *Proc. ESSDERC*, 373 (2004).
- [6] J.L. Autran, *et al.* Quantum-mechanical analytical modeling of threshold voltage in long-channel Double-Gate MOSFET with symmetric and asymmetric gates. *Nanotech. Proc.*, **2**, 163 (2004).
- [7] G. Baccarani, *et al.*, Compact Double-Gate MOSFET Model comprising quantum-mechanical and nonstatic effects. *IEEE Trans. Electron. Dev.*, **46**, 1656 (1999).
- [8] Balmos3D simulation code, L2MP-CNRS, (2003).